PNAS

Supporting Information for

Inhibition of FOXP3 by Stapled Alpha-Helical Peptides Dampens Regulatory T Cell Function

Katrina M. Hawley[1], Rachel J. Eclov[1], Mathew R. Schnorenberg[1, 3, 4], Yu Tian[4], Rhea N. Shah[1], Anika T. Thomas-Toth[1], Marie Fefferman[1], Gregory H. Bird[2], Loren D. Walensky[2], Matthew V. Tirrell[4,5*], James L. LaBelle[1*]

[1]Department of Pediatrics, Section of Hematology/Oncology, University of Chicago, Chicago, IL 60637, USA
[2]Department of Pediatric Oncology, Linde Program in Cancer Chemical Biology, Dana-Farber Cancer Institute, Boston, MA 02215, USA
[3]Medical Scientist Training Program, University of Chicago, Chicago, IL 60637, USA
[4]Pritzker School of Molecular Engineering, University of Chicago, Chicago, IL 60637, USA
[5]Argonne National Laboratory, Lemont, IL 60439

***Corresponding Authors:**

James L. LaBelle
900 East 57th Street, KCBD 5122
Phone: 773-702-6812
Email: jlabelle@peds.bsd.uchicago.edu

Matthew V. Tirrell
5640 South Ellis Avenue, Room 299C, Chicago, IL 60637
Phone: 773-834-2001
Email: mtirrell@uchicago.edu

This PDF file includes:

SI Material and Methods
Figures S1 to S9
Table S1
SI References

SI Materials and Methods

Recombinant Protein Constructs, Expression, and Purification.

Human ΔN FOXP3 (T182-P431) and LZCC (T182-M337) were cloned from FOXP3-pcDNA3.1 kindly provided by Anjana Rao (1) using Taq DNA polymerase (Qiagen) and primers listed below per the manufacturer's protocol. PCR fragments were ligated into pGEX4T1, and the vector's glutathione S-transferase tag was changed to a 6x-His tag using His primers (*SI Appendix*, Table S1) and a previously described around the horn PCR amplification scheme (2). BL21 bacteria expressing His_6-LZCC-pGEX4T1 (T182-M337) and His_6-Δ*N*-pGEX4T1 (T182-P431) were induced when optical density at 600 nm reached 0.6-0.8 with 1 mM isopropyl ß-D-1-thiogalactopyranoside for 6 h at 37 °C while shaking. Bacteria were pelleted using an ultracentrifuge and stored for future use in a −80 °C freezer. Bacterial pellets were suspended in base buffer (100 mM KCL, 20 mM Hepes, 10 μM ethylenediaminetetraacetic acid [EDTA], 10% glycerol, 20 mM imidazole, and 1 mM dithiothreitol [DTT]) and lysed with lysozyme (1 mg/mL) for 30 min. Pellets were then sonicated six times in 10 s on/off pulses at 4 °C. Nuclease (1:10,000) and protease inhibitors without EDTA were added for 15 min before lysate was clarified by centrifugation at 6,000 × *g* for 60 min. The remaining supernatant was incubated with Ni-nitrilotriacetic acid (NTA) resin for 1 h at 20 °C. The Ni-NTA resin was washed with base buffer (+30 mM imidazole). Protein was eluted from the Ni-NTA resin with base buffer (+500 mM imidazole) and purified by size exclusion on an ATKApure fast protein liquid chromatography machine using a Superdex 75 column (GE Lifesciences). Protein production was confirmed by sodium dodecyl sulfate-polyacrylamide gel electrophoresis separation followed by Coomassie staining to identify appropriately sized protein or by Western blot analysis using His antibody (Invitrogen No. MA1-21315) and quantified by extinction coefficient at 280-nm wavelength using a DeNovix DS-11 Spectrophotometer.

FPA.

Fluorescence polarization analyses were performed to measure binding of FITC-labeled SAHs to serially diluted recombinant ΔN or LZCC FOXP3 (max concentration 4 μg/mL) as previously described (3). Protein was incubated with 50 nM FITC-labeled native or stapled peptide in 1× PBS (pH 8) (final volume 200 μL) for 1-15 min at room temperature in a 96-well black flat-bottom plate (Nunc). Polarization values were measured at λ_{em} = 492 nm and λ_{ex} = 517 nm using a SpectraMax spectrometer (Molecular Devices). Polarization values were determined using the equation: $P = (Y - X)/(Y + X)$, where Y is vertical emission intensity and X is horizontal emission intensity. The fraction of peptide bound to protein was calculated using the equilibrium polarization value obtained for a given protein to which background-subtracted fluorescence polarization values were normalized. Binding curves, K_d values, and 95% CIs were determined utilizing Prism graphing software. The data were fit to a sigmoidal binding curve (four-parameter) that follows the equation $Y = \text{bottom} + (\text{top} - \text{bottom})/(1 + 10^{(\text{LogEC50} - X) \times \text{HillSlope}})$, as described on the Prism 6 website.

EMSAs.

Single-stranded oligonucleotides containing FOXP3-binding sites were annealed with their respective complementary strands and purified on 12% polyacrylamide gels as described (1). IR700-labeled FOXP3 probes (A'GT25, *SI Appendix*, Table S1) were incubated for 15 min at room temperature with 50-100 pmoles of recombinant ΔN FOXP3 along with DMSO, peptide, 200× unlabeled oligo, or anti-FOXP3 (Abcam Ab248) antibody. The binding buffer contained 12 mM Hepes (pH 7.5), 100 mM NaCl, 1 mM DTT, 1 mM EDTA, 12% glycerol, and 20 μg/mL poly(dI)-poly(dC). DNA-protein complexes were then separated by electrophoresis on a 10% polyacrylamide, Tris-borate-EDTA gel and were imaged using an Odyssey Imager (Li-Cor).

SPR.

Purified LZCC, ΔN, or full-length FOXP3 (Origene TP317580) was associated to a Series S CM5 chip (Cytiva No. 29104988) through covalent bonding. 50 mM NaOH was used to remove the protective layer on the CM5 chip, followed by protein immobilization with 1-ethyl-3-(3-dimethylaminopropyl)carbodiimide), N-hydroxysuccinimide, and ethanolamine per the manufacturer's directions. The amount of desired protein bound was based on calculating R_{lig} with a target R_{max} of 50 response units. Following peptide immobilization, increasing concentrations of peptides were washed over the chip for a 20-s association time and 30-s dissociation time. Kinetic curves were calculated using a two-state reaction global fit, and

kinetic constants were used to calculate K_D. The reference sample was a buffer-only sample flowed over immobilized protein.

Confocal Fluorescent Microscopy for Peptide Penetration.
Human iTreg cells were treated with 0-5 μM FITC peptide for 4 h in OptiMEM, washed twice with PBS, fixed in 2% paraformaldehyde for 15 min at room temperature, and stained with Hoechst 33342 dye at a 1:1,000 dilution in PBS for 10 min at room temperature. Cells were reconstituted in PBS at a concentration of 2 million/mL and 100 μL (200,000 cells) and spun onto slides using a Thermo Scientific Cytospin 4 at 400 rpm for 2 min. Slides were then imaged using a Leica SP5 laser confocal microscope. Post acquisition processing (multichannel overlay) was performed using ImageJ software (NIH). The results are representative of images taken from multiple fields across the same slide in at least three biological replicates.

Viability Assays.
Murine thymocytes were freshly isolated and plated at 50,000 cells/well. The cells were incubated with increasing concentrations of peptides, DMSO, or positive control (1% Triton X-100) for LDH release assays in 200 μL OptiMEM for 4 h. Cells were pelleted and media extracted for colorimetric analysis using a cytotoxicity detection kit following the manufacturer's protocol (Roche). Data were background subtracted and normalized to the positive control in order to measure % cytotoxicity.

To measure apoptosis, cells were stained with annexin V-APC from an Annexin V Apoptosis Detection Kit following the manufacturer's protocol (eBiosciences). Immediately prior to analysis on a LSRII cytometer (BD Biosciences), 2 μL of PI (Life Technologies) was added to each tube.

Peptide Treatments.
T cells were washed in PBS and then suspended in OptiMEM with 100 nM to 10 μM of peptide or DMSO. Cells were treated for 2 h at 37 °C in serum-free conditions and then either left unstimulated or stimulated with 10 ng/μL phorbol 12-myristate 13-acetate + 0.5 μM ionomycin in complete media for 4 h prior to extracting RNA for qPCR. Cells were treated for 2 h at 37 °C in serum-free conditions and then stimulated for 22 h with CD3/CD28 Dynabeads in complete media prior to flow cytometric analysis for protein expression.

RNA Isolation and cDNA Preparation.
Following relevant peptide treatments as indicated above, cells were lysed with TRIzol (Life Technologies) and total RNA was isolated from each treatment condition using the Direct-zol RNA MiniPrep kit (Zymo Research) per manufacturer's instructions and quantified by DeNovix DS-11 Spectrophotometer. RNA was either saved for RNA sequencing or converted to complementary DNA (cDNA) for qRT-PCR. RNA from each biological replicate (1 μg) was converted to double-stranded cDNA using the SuperScript III first-strand synthesis reverse transcription kit (Invitrogen) per the manufacturer's directions.

qRT-PCR.
qRT-PCR was performed using TaqMan Master Mix and Gene Expression Probes (Applied Biosystems) for each of the following genes: *Foxp3*: Mm00475162, *Il2ra*: Mm01340213, and *Ubc*: Mm02525934. Samples were run on the 7500 Fast Real-Time PCR System (Applied Biosciences). Data were analyzed with the ExpressionSuite software utilizing the $\Delta\Delta C_T$ method with Ubc as the housekeeping gene and DMSO-treated cells as reference samples. Data shown are means of technical triplicates plotted as a single plot for three biological replicates.

Flow Cytometric Analysis.
Cells were acquired and treated as described above. The following antibodies were used for staining at a dilution of 1:100 in PBS in the dark at 4 °C for 30 min: CD4 PE (BD No. 553730), CD25 APC (BD No. 557192), Live/Dead APC-Cy7 (ThermoFisher No. L34975). For intracellular staining of FOXP3 and cytokines, cells were fixed and permeabilized with the FOXP3 Fixation/Permeabilization kit (eBioscience) per the manufacturer's protocol. After fixation and permeabilization, cells were stained with a FOXP3 FITC antibody (Invitrogen No. 11–5773-82) at 1:50 in permeabilization buffer for a minimum of 1 h on ice.

Samples were analyzed using a LSRII cytometer (BD) or FACSAria (BD). Data analysis was performed using FlowJo software (Tree Star).

Ex Vivo Suppression Assays.
C57BL/6 mice were sacrificed, and splenocytes were isolated by physical disruption as described above. Splenocytes were $CD3^+$ T cell depleted utilizing the CD3e Microbead kit per manufacturer's directions (Miltenyi Biotec No. 130–094-973). CD3-depleted splenocytes were then irradiated with 3,000 rads gamma irradiation. Following Tcon cell and Treg cell isolation via fluorescence-activated cell sorting as described above, Tcon cells were labeled with CellTrace Violet (ThermoFisher No. C34557) per the manufacturer's protocol. Treg cells were then serially diluted down a 96-well U-bottom plate (50,000 cells to 3,125 cells per well) and cocultured with 50,000 labeled Tcon cells, 250,000 irradiated splenocytes, and soluble CD3 antibody at 1 μg/mL (BioXCell No. BE0002). The cells were stimulated for 3 d before staining with APC-Cy7 Live/Dead (ThermoFisher No. L34975) per manufacturer's protocol, along with antibodies CD4-PE (BD No. 553730) and CD25-APC (BD No. 557192) at a 1:100 dilution in PBS. Cells were analyzed via flow cytometry and analyzed on FlowJo software (Tree Star).

RNA Sequencing and Data Analysis.
Library preparation and sequencing were performed by the University of Chicago Genomics Facility. One hundred base pair paired-end reads for each sample were generated using the HiSEQ4000 (Illumina, San Diego, CA). Alignment to the murine genome (mm10) was performed using Tophat and Bowtie. Differential expression analysis was performed using EdgeR, and data were filtered to exclude genes with counts per million (CPM) <2 in three or more samples. GSEA was performed using the GSEA portal (http://www.broad.mit.edu/GSEA/). Each gene set was queried for enrichment within the expression profile generated by comparing DMSO- and SAH-treated cells. GSEA was performed with the following parameters: probe set collapse = false; phenotype = SAH versus DMSO; permutation = sample, permutations = 1,000. Gene set size: $50 < n < 1{,}000$, utilizing diff_of_classes. Samples are plotted in columns and the genes in rows.

Statistical Statements.
A one-way ANOVA test with multiple comparisons was used to evaluate statistically significant changes between SAH-treated cells in qRT-PCR analyses where each dose group was evaluated for statistical significance against the other groups. Plots were created using Prism 7 (GraphPad Software). Expression data were depicted by RQ Min/Max with a 95% confidence level using the ExpressionSuite Software (Thermo Fisher/Life Technologies). Statistical significance was defined as $P < 0.05$ or as otherwise indicated.

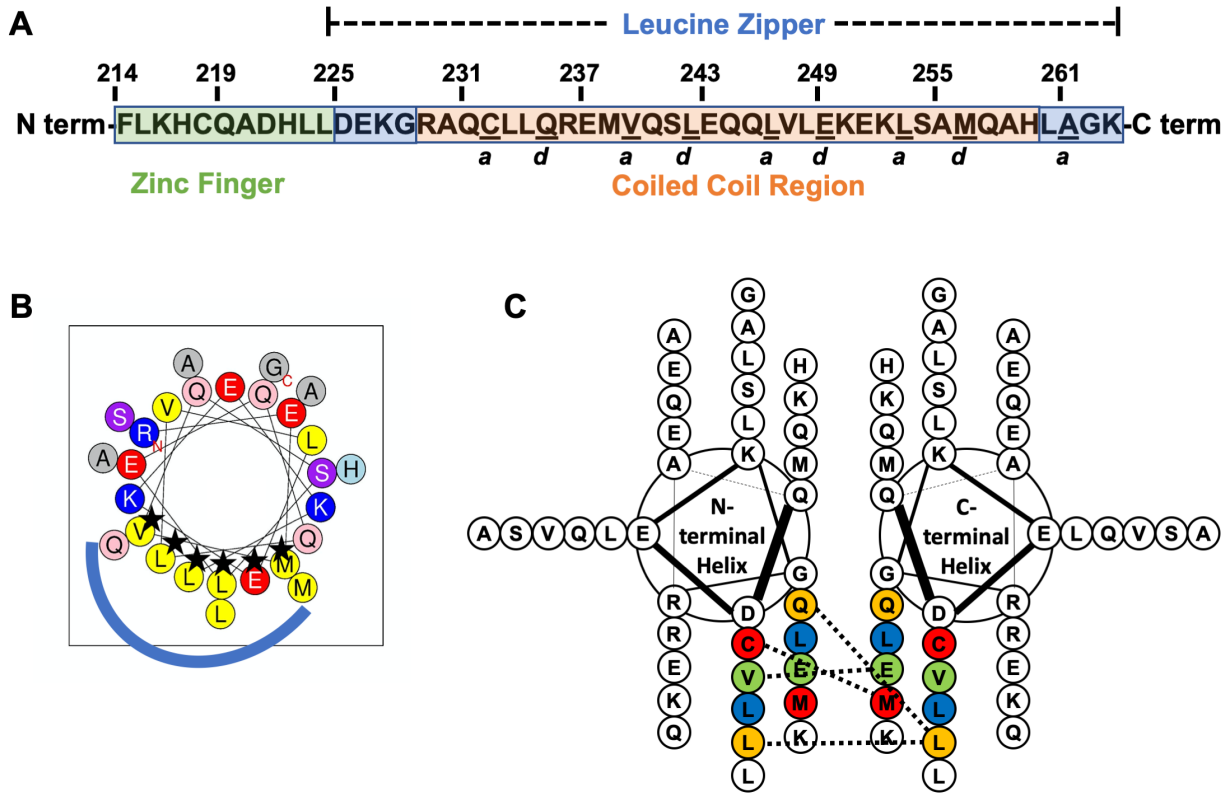

Fig. S1. Strategic design of staple positions for FOXP3-targeting SAHs in relation to the FOXP3:FOXP3 interface. (A) Human FOXP3 sequence. Residues F214-K263 represent the entirety of a helix constituting the zinc finger (F214-L224; shown in green) and leucine zipper (D225-K263; shown in blue) regions. Within the leucine zipper, the coiled-coil (R229-H259; shown in orange), represents an area that is highly conserved between human and murine FOXP3. Underlined residues indicate a and d core residues, which bind each other on an identical anti-parallel helix, and are key contact points for homodimerization. The homodimerized FOXP3 helix is labeled according to the color codes in the sequence above. (B) Helical wheel plot shows the relative position of amino acids looking down the barrel of the helix. Positively charged amino acids (blue), negatively charged amino acids (red), and hydrophobic amino acids (yellow) are indicated. The more hydrophobic side of the helix constitutes the majority of the residues constituting the FOXP3:FOXP3 interacting face (blue half circle). Residues of *a* and *d* resonance are starred. (C) Two helical wheel plots are shown with residues of *a* and *d* resonance color-coded as defined above. Interactions between individual amino acids on oppositely-oriented FOXP3 helices are indicated by a dotted line.

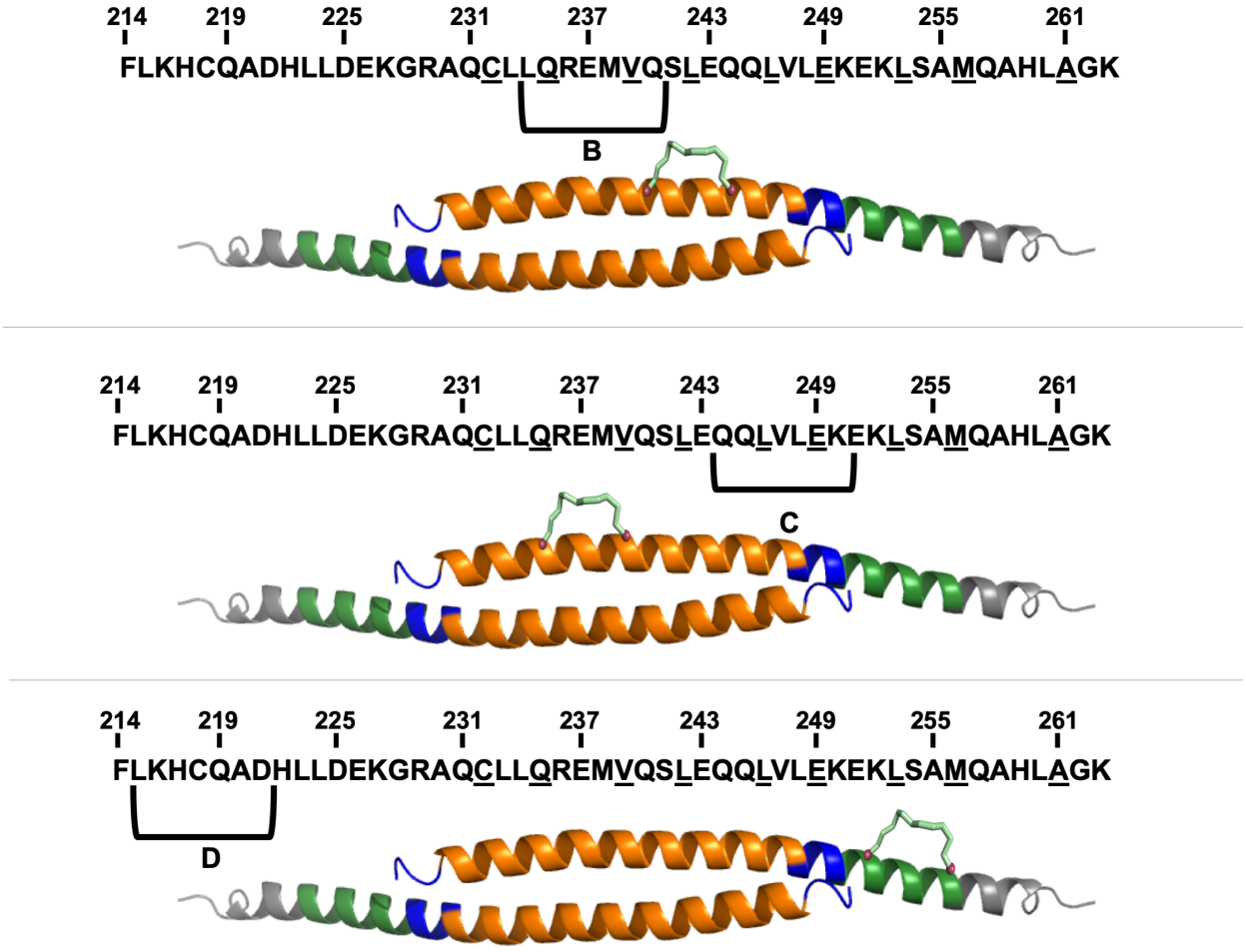

Fig. S2. Position of hydrocarbon staples screened in SAH-FOXP3 design. Three staple positions (B, C, and D) were utilized in initial SAH design. Each of the staples faces away from the FOXP3 dimerization interface and are positioned either N-terminally, C-terminally, or centered with respect to the middle of the peptide length.

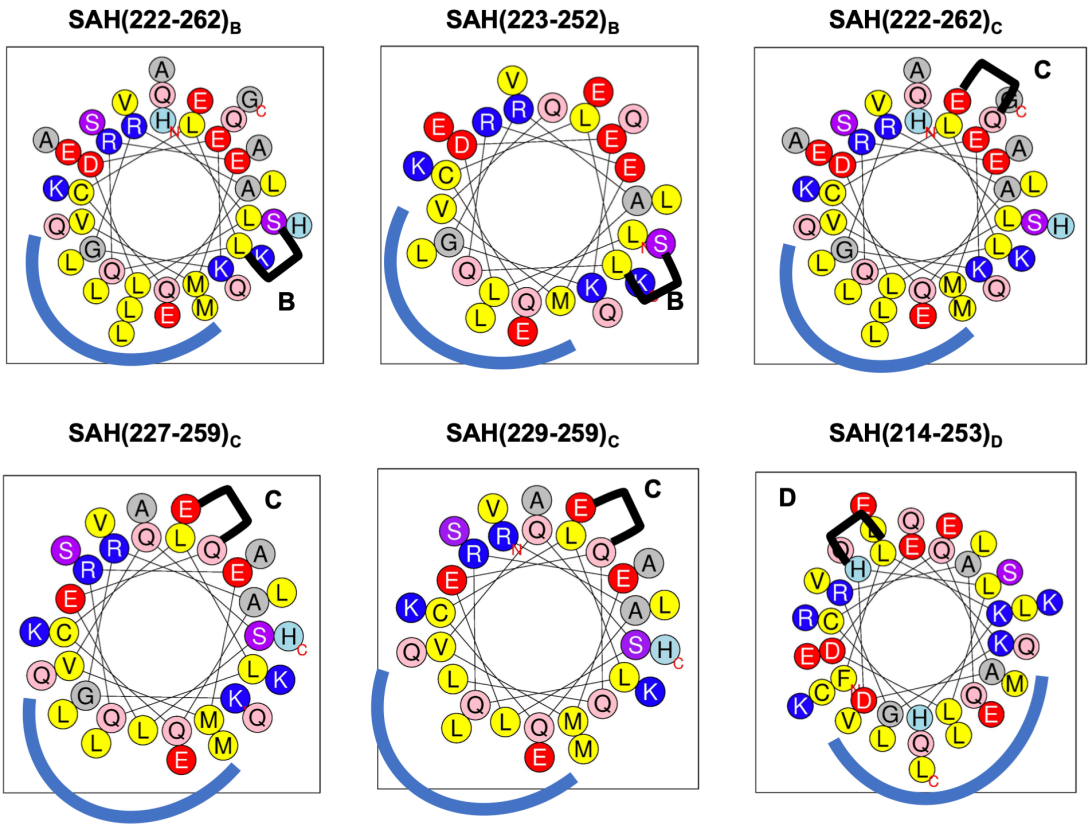

Fig. S3. Visualization of staple positions of SAHs targeting FOXP3 in relation to FOXP3:FOXP3 interface. Helical wheel plots indicate the relative position of amino acids looking down the barrel of the helix. Positively charged amino acids (blue), negatively charged amino acids (red), and hydrophobic amino acids (yellow) are indicated. The more hydrophobic side of the helix constitutes the majority of the residues on the interacting face (blue half circle). Helical wheel plots for screened single-stapled FOXP3-targeting SAHs are shown with staple positions labeled and indicated. Staples are placed either opposite the interacting face to avoid interference, or immediately adjacent to this interacting area in an effort to extend the naturally occurring hydrophobic interface.

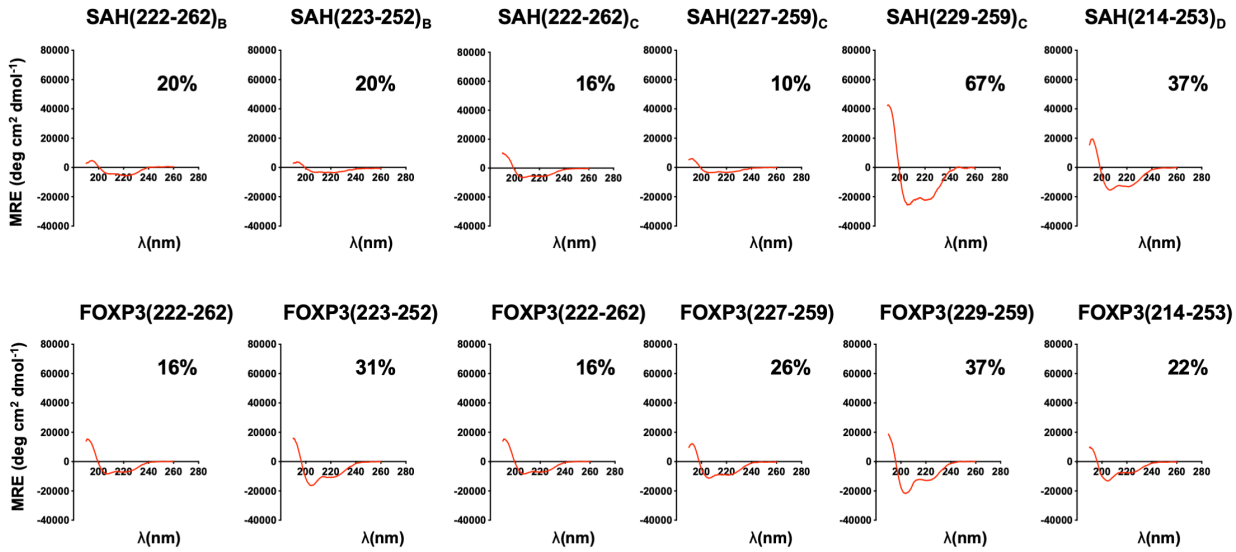

Fig. S4. Circular dichroism indicates sequence and staple position differences greatly impact alpha-helicity of SAHs. Circular dichroism of FOXP3-targeting SAHs and native unstapled peptides demonstrate that sequence and staple position result in radically different measured alpha-helicities as calculated by the ratio of peaks at wavelength 208 and 222.

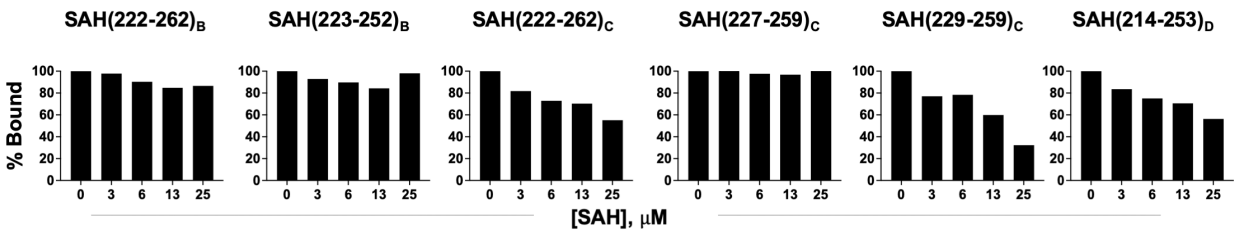

Fig. S5. Quantification of EMSA-based screening of peptides targeting FOXP3.
Quantification of Electrophoretic mobility shift assays (EMSAs) depicted in Fig. 2B demonstrate that altering the sequence and staple position in SAHs targeting FOXP3 lead to substantially different capacities to block FOXP3 binding to a cognate DNA oligonucleotide probe.

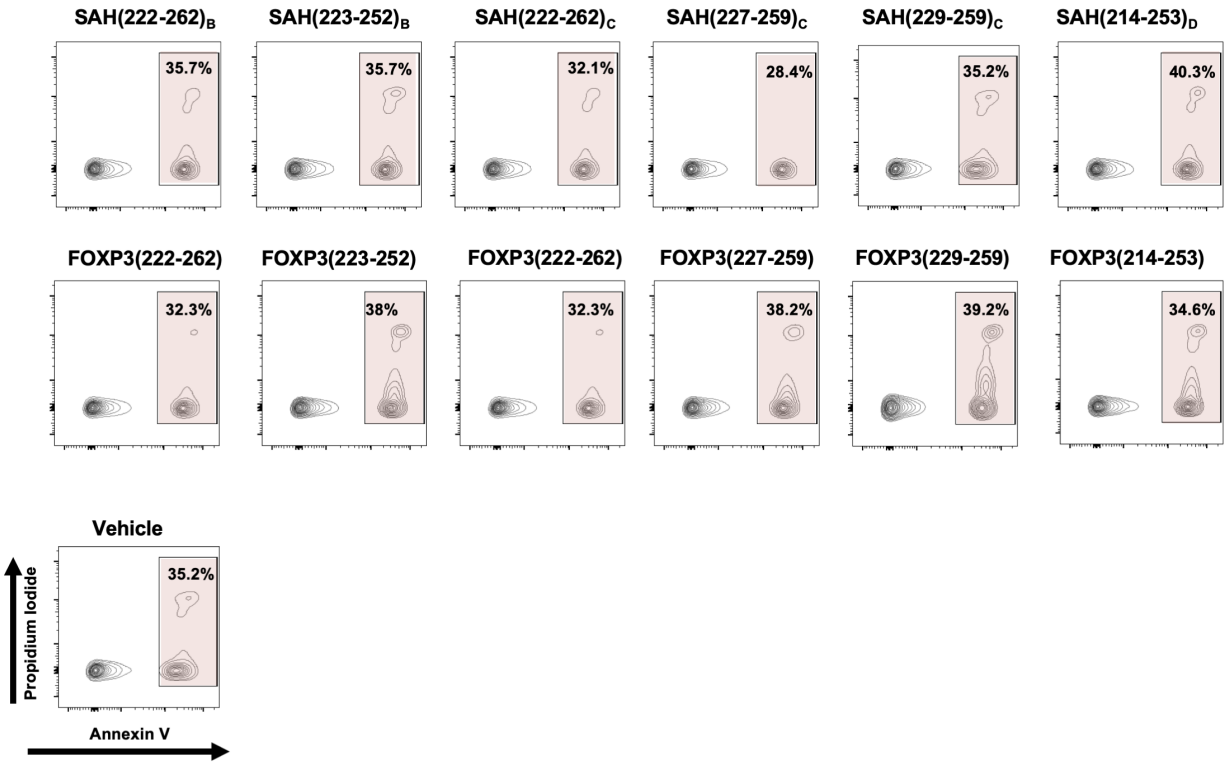

Fig. S6. SAHs targeting FOXP3 are non-toxic to T cells. Apoptosis as measured by Annexin V (APC) and Propidium Iodide (PI) staining via flow cytometry in T cells treated with SAHs. Vehicle treated controls are shown below their stapled analogs. All compounds exhibited similar levels of apoptosis as vehicle control-treated cells.

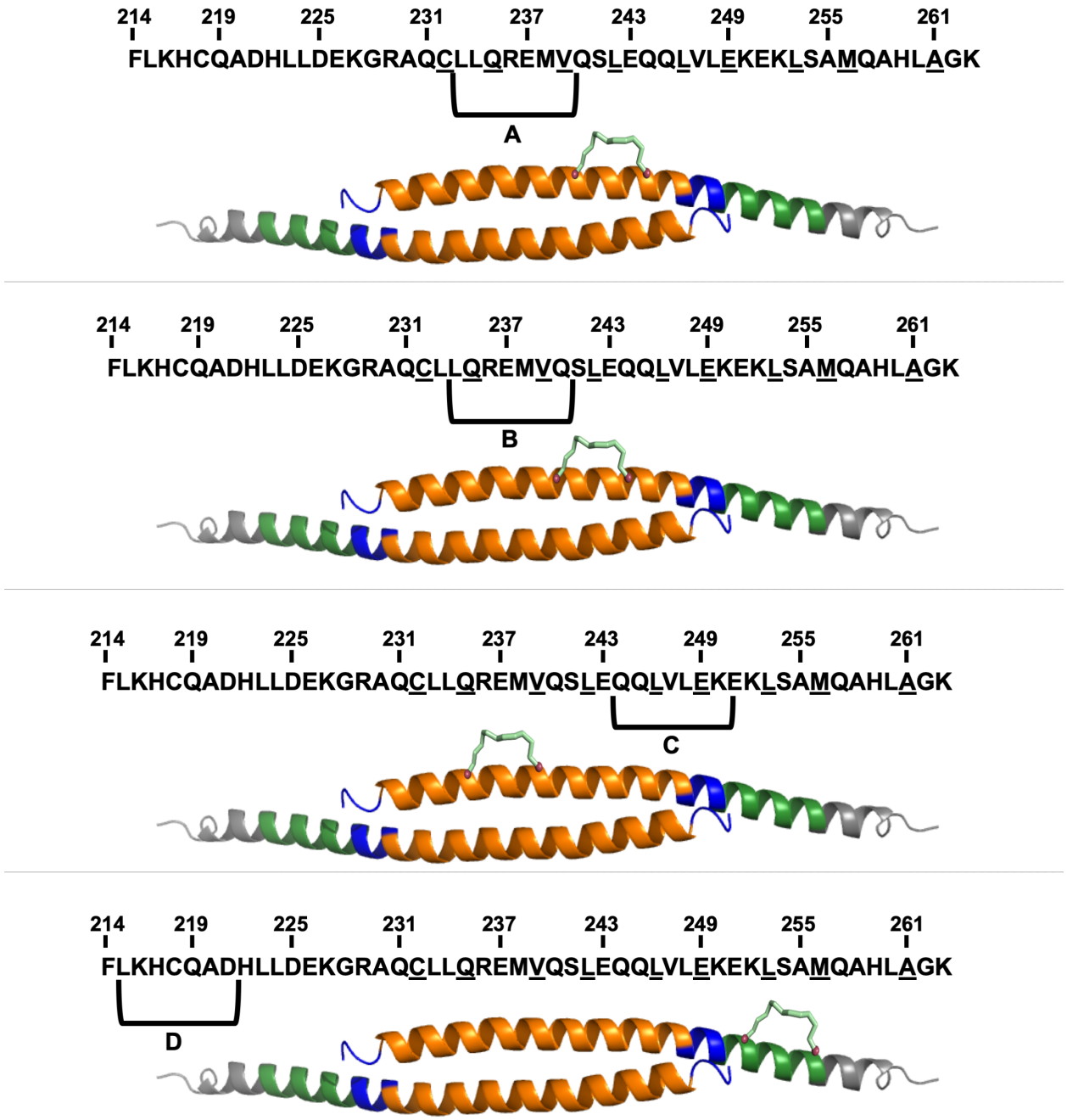

Fig. S7. Staple positions tested in analogs of SAH(229-259)c. Four staple positions (A, B, C, and D) were utilized in SAH design. Each of the staples faces away from the dimerization interface and are positioned either N-terminally, C-terminally, or centered with respect to the middle of the peptide length. A and B staple positions are used specifically in the double-stapled iterations.

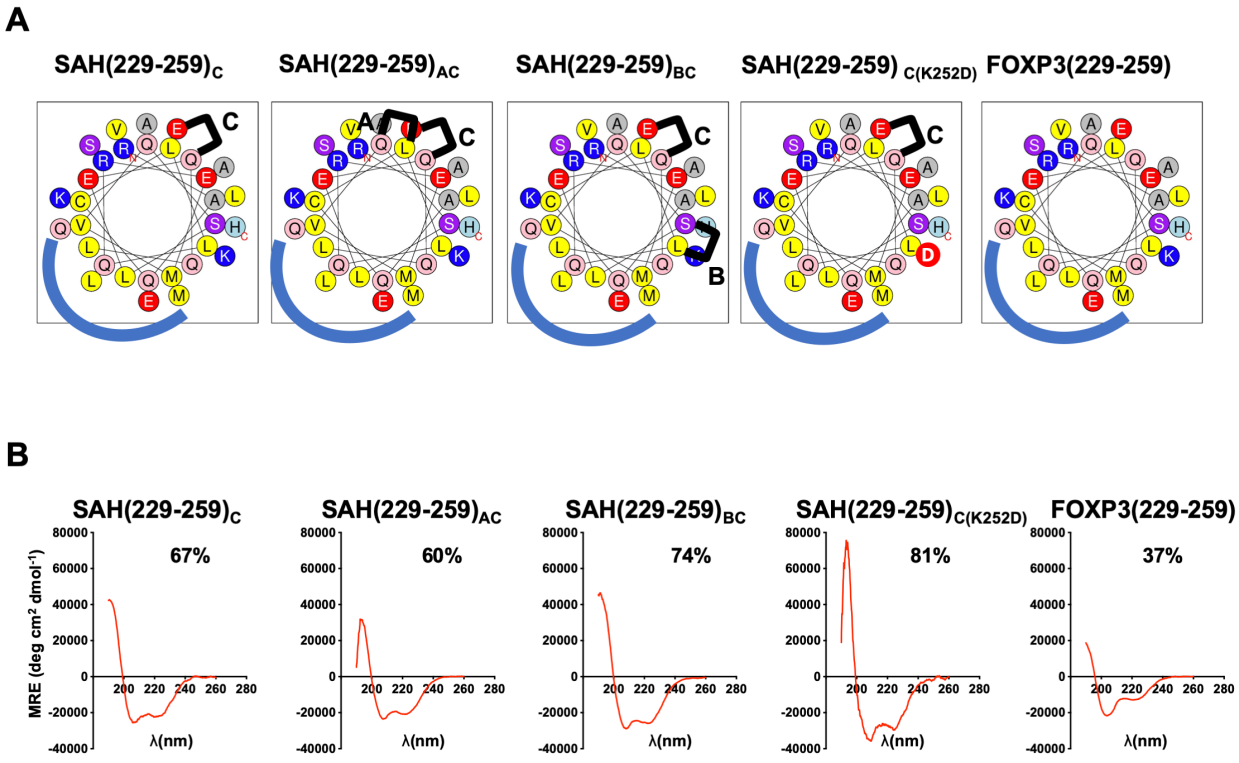

Fig. S8. Characterization of SAH(229-259)$_C$ iterations. (A) Helical wheel plots show the relative position of amino acids looking down the barrel of the helix. Positively charged amino acids (blue), negatively charged amino acids (red), and hydrophobic amino acids (yellow) are indicated. The more hydrophobic side of the helix constitutes the majority of the residues on the interacting face (blue half circle). Helical wheel plots for SAH(229-259)$_C$ analogs are shown with staple positions labeled and indicated. Staples are placed either opposite the interacting face to avoid interference, or immediately adjacent to this interacting area in an effort to extend the naturally occurring hydrophobic interface. (B) Circular dichroism of SAH(229-259)$_C$ iterations demonstrate that double-stapling alone does not necessarily confer improved α-helicity as measured by the ratio of peaks at wavelength 208 and 222.

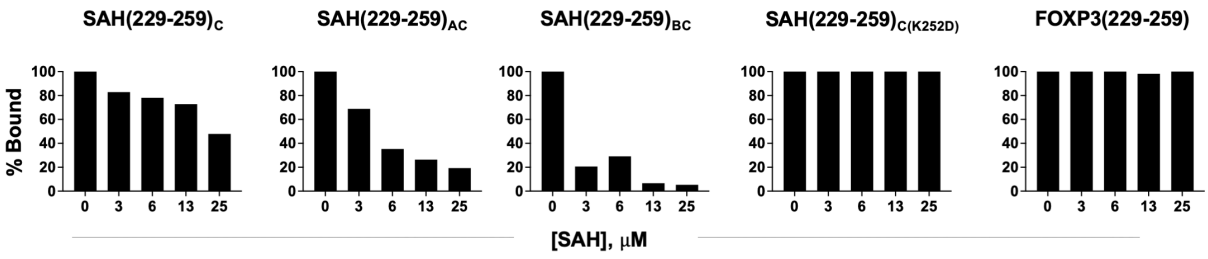

Fig. S9. Quantification of EMSAs of SAH(229-259)$_C$ derivatives.
Quantification of Electrophoretic mobility shift assays (EMSAs) depicted in Fig. 4B demonstrate observable reduction in FOXP3 binding to a consensus DNA oligonucleotide probe following treatment with SAH(229-259)$_C$ derivatives but not native peptide or point mutant control.

Primer/Probe Name	Sequence 5' to 3'
T182 Forward	TATAGAATTCACCCTTTCGGCTGTGCC
M337 Reverse	TCGACTCGAGTGTTGTGGAACTTGAAGTAG
P431 Reverse	TATACTCGAGAGGTGTAGGGTTGGAACACC
His Forward	CTGGTTCCGCGTGGATCCCCGGAATTC
His Reverse	ATGGTGATGGTGATGGTGCATGAATACTGTTTCCTGTG
delE251 SDM F	GGAGAAGAAGCTGAGTGCCATGCAGG
delE251 SDM R	CAGCTGGTGCTGGGGAGAAGAAGCTG
Mutant K251D F	CTGGAGAAGGAGGATCTGAGTGCCATG
Mutant K251D R	CATGGCACTCAGATCCTCCTTCTCCAG
EMSA A'GT25	CAAGGTAAACAAGACAACGTAAACAA

Table S1. Primer and EMSA probes.

References

1. J. Koh *et al.*, Regulatory (FoxP3(+)) T cells and TGF-beta predict the response to anti-PD-1 immunotherapy in patients with non-small cell lung cancer. *Sci Rep* **10**, 18994 (2020).
2. H. Liu, J. H. Naismith, An efficient one-step site-directed deletion, insertion, single and multiple-site plasmid mutagenesis protocol. *BMC Biotechnol* **8**, 91 (2008).
3. J. L. LaBelle *et al.*, A stapled BIM peptide overcomes apoptotic resistance in hematologic cancers. *J Clin Invest* **122**, 2018-2031 (2012).